JOURNAL OF CATALYSIS **172,** 24–33 (1997)
ARTICLE NO. CA971828

State of Platinum in Zirconium Oxide Promoted by Platinum and Sulfate Ions

Tetsuya Shishido,* Tsunehiro Tanaka,† and Hideshi Hattori*,[1]

*Center for Advanced Research of Energy Technology, Hokkaido University, Sapporo 060, Japan; and †Division of Molecular Engineering, School of Engineering, Kyoto University, Kyoto 606, Japan

Received November 1, 1996; revised July 7, 1997; accepted July 14, 1997

The state of platinum in the zirconium oxide promoted by platinum and sulfate ions ($Pt/SO_4^{2-}-ZrO_2$) has been investigated by means of Pt L-edge XAFS (X-ray absorption near edge structure (XANES)/extended X-ray absorption fine structure (EXAFS)). The XANES shows that Pt is electron-deficient even after reduction with hydrogen. Fourier transforms of k^1 and k^3-weighted EXAFS results indicate the presence of Pt–O and Pt–Pt pairs in the $Pt/SO_4^{2-}-ZrO_2$. On the basis of XAFS, the reported contradictory results that Pt is metallic by XRD analysis and Pt is in a cationic state by XPS are explained by the model that oxidized platinum particles with a metallic core are present in the $Pt/SO_4^{2-}-ZrO_2$ even after the reduction. © 1997 Academic Press

INTRODUCTION

It has been reported by several groups that the addition of platinum to zirconium oxide promoted by sulfate ions ($SO_4^{2-}-ZrO_2$) enhances catalytic activity in the skeletal isomerization of alkanes without deactivation when the reaction is carried out in the presence of hydrogen (1–3). The high catalytic activity and small deactivation can be explained by both the elimination of the coke by hydrogenation and/or hydrogenolysis (1) and the generation of protonic acid sites from molecular hydrogen on the catalysts (2, 3). The platinum species in the $Pt/SO_4^{2-}-ZrO_2$ exhibit a unique catalytic property different from that of metallic platinum; the platinum species neither show appreciable activities for hydrogenation and hydrogenolysis (2, 4), nor adsorb CO (5). These results suggest that the state of platinum is different from the metallic state as observed for a usual supported platinum. The state of platinum, however, has been left unclear and is still a matter of controversy (6). Ebitani *et al.* reported that Pt is mainly in an oxidized state with some metallic phase inside on the basis of X-ray photoelectron spectroscopy (XPS), IR of adsorbed CO and temperature-programmed reduction (TPR) techniques (5, 7–9). Paál *et al.* reported that Pt is sulfided in the activated catalysts (10). Iglesia *et al.* proposed that the platinum is present as a metal sulfide; thus, the platinum sulfide provides hydrogenation/dehydrogenation activity as well as a site for spillover hydrogen (11). On the basis of XPS, XRD (12), and TPR (13), Sayari and Dicko proposed that Pt is metallic, even after calcination in air.

X-ray absorption near edge structure (XANES) and extended X-ray absorption fine structure (EXAFS) can provide us with information about the electronic structure and local environment in the immediate vicinity of the absorbing atom without the stringent requirement of long-range structural order (14). Thus, these spectroscopic techniques are useful for characterization of highly dispersed supported metals (15–18). The sharp and narrow absorption bands at both L_3 and L_2 X-ray absorption edges, which are called white lines (19), correspond to the electronic transition from $2p_{3/2}$ and $2p_{1/2}$ core level states, respectively. The final vacant *d* states for L_3 edge are both $d_{3/2}$ and $d_{5/2}$ levels of the absorption atom, and that for L_2 edge is $d_{3/2}$ level (19, 20). Lytle *et al.* have reported that the magnitude (intensity) of the platinum L_3 X-ray absorption spectra is concerned to the *d*-electron valences (21) and the chemical environment (22). Mansour *et al.* (23) have developed a quantitative evaluation of the number of holes in the *d* bands of the dispersed platinum particles by using both L_3 and L_2 X-ray absorption edges. According to the Mansour's method, the total number of unoccupied *d* states (h_T) can be expressed by combination of the normalized areas of the L_3 and L_2 edges X-ray absorption, in principle. This method has been applied to elucidation of the electronic states of the platinum supported on TiO_2 (15), Al_2O_3 (24), and SiO_2 (24).

In the present study, we carried out XAFS experiments for Pt L-edge absorption to elucidate the state of platinum supported on $SO_4^{2-}-ZrO_2$.

EXPERIMENTAL METHODS

Catalyst Preparation

The sulfate ion-treated $Zr(OH)_4$ ($SO_4^{2-}-Zr(OH)_4$) was prepared by the impregnation of $Zr(OH)_4$ with 1*N* H_2SO_4

[1] Corresponding author. E-mail: hattori@carbon.caret.hokudai.ac.jp.

0021-9517/97 $25.00

aqueous solution followed by filtration and drying at 383 K. The $Zr(OH)_4$ was obtained by hydrolysis of $ZrOCl_2\ 8H_2O$ (Wako Pure Chemical) with 25% NH_4OH aqueous solution followed by filtration. The final value of pH was ca 8.0. The obtained gel was washed with distilled water until no Cl^- ions could be detected. The $SO_4^{2-}-ZrO_2$ was obtained by calcination of the $SO_4^{2-}-Zr(OH)_4$ at 873 K. The $Pt/SO_4^{2-}-ZrO_2$ sample (Pt 0.5 wt%) was prepared by impregnation of the $SO_4^{2-}-Zr(OH)_4$ with H_2PtCl_6 aqueous solution followed by drying at 383 K and calcination at 873 K in air.

XANES/EXAFS

X-ray absorption experiments were carried out at Photon Factory in National Laboratory for High Energy Physics (KEK-PF), Tsukuba, Japan, on BL7C station with apparatus operated in the fluorescence and transmission modes with double-crystal Si(111) monochrometer. Ring energy was 2.5 GeV. X-ray beam height is 1.0 mm at 25 m from X-ray source. Energy was calibrated with Cu K-edge absorption (8981.0 eV). Energy step of measurement in XANES region was 0.3 eV.

To obtain the degree of uncertainty in the determination of the structural parameters from EXAFS data, the experiment was performed on platinum foil (thickness 10 μm) and PtO_2 as reference materials of known structure. The oxidized sample was obtained by calcination in air at 873 K for 3 h. The reduced sample was obtained by heating in a hydrogen flow at 623 K for 2 h and cooled to room temperature in the presence of hydrogen followed by evacuation for 15 min. The reduced sample was handled under an inert condition during the X-ray experiment to avoid oxidation.

Analysis of EXAFS Data

The oscillatory part of the absorption coefficient as a function of the X-ray photon energy (E) was extracted as described elsewhere (25). Normalization of EXAFS oscillation was performed by fitting the background absorption coefficient (μ_0) around the energy region 35–50 eV higher than the absorption edge with the smoothed absorption of an isolated atom (McMaster type function, $CE^{-2.75}$ (26)). This normalization method has been previously reported in detail (27).

Fourier transformation (FT) of normalized EXAFS oscillation was performed over the range $3.5 < k < 13.5$ Å^{-1} for k^3-weighted EXAFS and the range $4.0 < k < 12.0$ Å^{-1} for k^1-weighted EXAFS in order to obtain the radial structure function (22, 28). Both k^1 and k^3 weighting analysis is a prerequisite, since the k-dependence of the backscattering amplitude of low Z elements (e.g., O) is different from that of high Z elements (e.g., Pt). The backscattering amplitude of the low Z elements becomes very small above $k = 10$ Å^{-1}, in comparison with the amplitude of high Z scatters, which is still significant at higher k values (29). Application of only k^3-weighting analysis in systems containing both high and low Z scatters leads to an underestimation of the contribution of the low Z elements and overestimation of the contribution of the high Z elements.

The coordination number of scatters (N), the distance between an absorbing atom and scatters (R), and the Debye–Waller factor were estimated by curve-fitting analysis with the inverse FT, assuming single scattering (14). The ranges of R with the inverse FT were 1.2–3.4 Å for FT of k^3-weighted EXAFS and 1.0–3.3 Å for FT of k^1-weighted EXAFS. The reference parameters (phase shift and back scattering amplitude) for Pt–Pt shell and Pt–O shell were taken from those for Pt foil and PtO_2, respectively.

Data reductions were carried out with the FACOM M-780 computer system of the Data Processing Center of Kyoto University.

RESULTS

XANES

Figure 1 shows the normalized Pt L_3 and L_2-edge XANES for $Pt/SO_4^{2-}-ZrO_2$ calcined at 873 K in air for 3 h (oxidized $Pt/SO_4^{2-}-ZrO_2$) and that subsequently reduced with hydrogen at 623 K for 1.5 h (reduced $Pt/SO_4^{2-}-ZrO_2$). The XANES of Pt foil and PtO_2 are also included. The absorption edges shown in Fig. 1 have been already normalized as described in the experimental section. The energy offset was taken to be the position of each edge by subtraction of 11560 eV for Pt L_3 edge and 13270 eV for Pt L_2 edge. Large areas of both L_3 and L_2 absorption edges for PtO_2 are due to the vacancy in the 5d orbital of Pt atoms. The areas of L_3 and L_2 absorption edges for the calcined $Pt/SO_4^{2-}-ZrO_2$ is larger than those for Pt foil, showing that the Pt in the calcined $Pt/SO_4^{2-}-ZrO_2$ is electron deficient. The areas of L_3 and L_2 absorption edges decreased on hydrogen treatment, suggesting that a part of platinum is reduced. However, the areas for the reduced $Pt/SO_4^{2-}-ZrO_2$ is larger than those of Pt foil. The areas of L_3 and L_2 absorption edges indicate that the order of electron deficiency is PtO_2 > the oxidized $Pt/SO_4^{2-}-ZrO_2$ > the reduced $Pt/SO_4^{2-}-ZrO_2$ > Pt foil. The oscillation by XANES which appears at high energy side (above ca 15 eV from the absorption edge) is observable for both oxidized $Pt/SO_4^{2-}-ZrO_2$ and reduced $Pt/SO_4^{2-}-ZrO_2$. The oscillations of both oxidized $Pt/SO_4^{2-}-ZrO_2$ and reduced $Pt/SO_4^{2-}-ZrO_2$ are similar to that of Pt foil, but intensities are much weaker than that of Pt foil.

Reproduced Pt L_3-edge XANES obtained by fitting Pt L_3-edge XANES of Pt foil and PtO_2 are shown in Fig. 2. In the case of the oxidized $Pt/SO_4^{2-}-ZrO_2$, XANES is well reproduced by the sum of that of Pt foil $\times$ 0.6 and that of $PtO_2 \times 0.4$. This result indicates that about 60% of the platinum has been reduced already to Pt metal by calcination

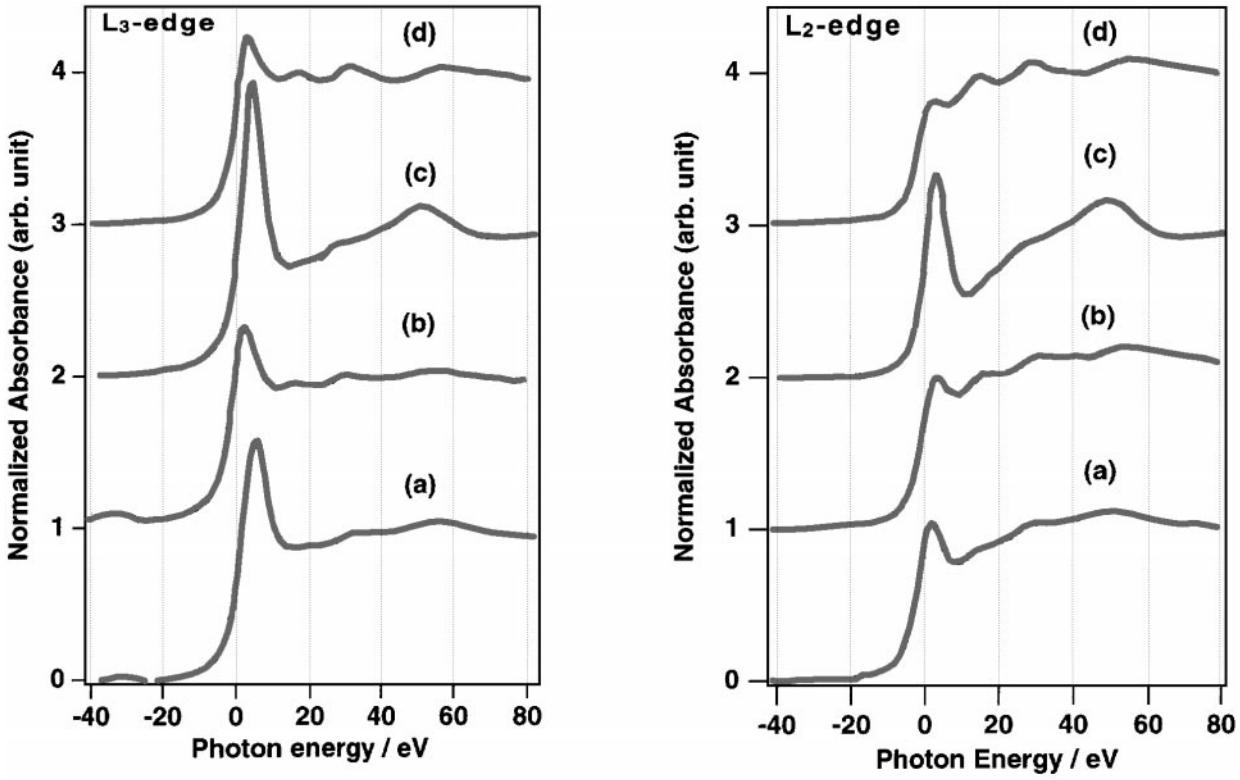

FIG. 1. Normalized Pt L_3 and L_2-edge XANES of (a) oxidized Pt/SO_4^{2-}–ZrO_2, (b) reduced Pt/SO_4^{2-}–ZrO_2, (c) PtO_2, and (d) Pt foil.

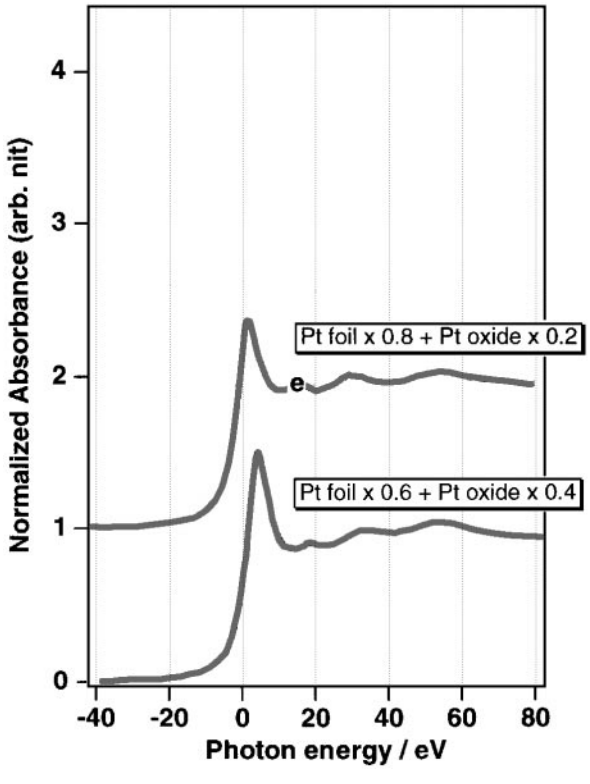

FIG. 2. Reproduction of Pt L_3-edge XANES from PtO_2 and Pt foil.

at 873 K. On the other hand, XANES is reproduced by the sum of that of Pt foil × 0.8 and that of PtO_2 × 0.2 in the case of the reduced Pt/SO_4^{2-}–ZrO_2. This result indicates about 80% of the platinum was metallic. These results suggest that a part of the platinum was converted to the metallic state by the hydrogen treatment at 623 K for 2 h. The information from XANES is not sufficient to identify the state of Pt because we cannot assert whether Pt is present as electron-deficient metal particles or as a mixture of Pt cation and Pt metal.

EXAFS

Pt L_3-edge k^3-weighted EXAFS (k versus $k^3\chi(k)$) and k^1-weighted EXAFS (k versus $k^1\chi(k)$) are shown in Figs. 3 and 4, respectively, for oxidized Pt/SO_4^{2-}–ZrO_2, reduced Pt/SO_4^{2-}–ZrO_2, Pt foil, and PtO_2. The k value is the photoelectron wave vector and the $\chi(k)$ value is the experimental Pt L_3-edge EXAFS function. The EXAFS oscillations of both oxidized Pt/SO_4^{2-}–ZrO_2 and reduced Pt/SO_4^{2-}–ZrO_2 are similar to that of Pt foil. The EXAFS spectra suggest that most of the platinum atoms on the SO_4^{2-}–ZrO_2 are in the metallic state.

Figure 5 shows the Fourier transforms of Pt L_3-edge k^3-weighted (emphasizing the Pt–Pt contributions) EXAFS of the Pt/SO_4^{2-}–ZrO_2, Pt foil, and PtO_2. The Fourier transform of Pt L_3-edge k^3-weighted EXAFS for Pt foil exhibits

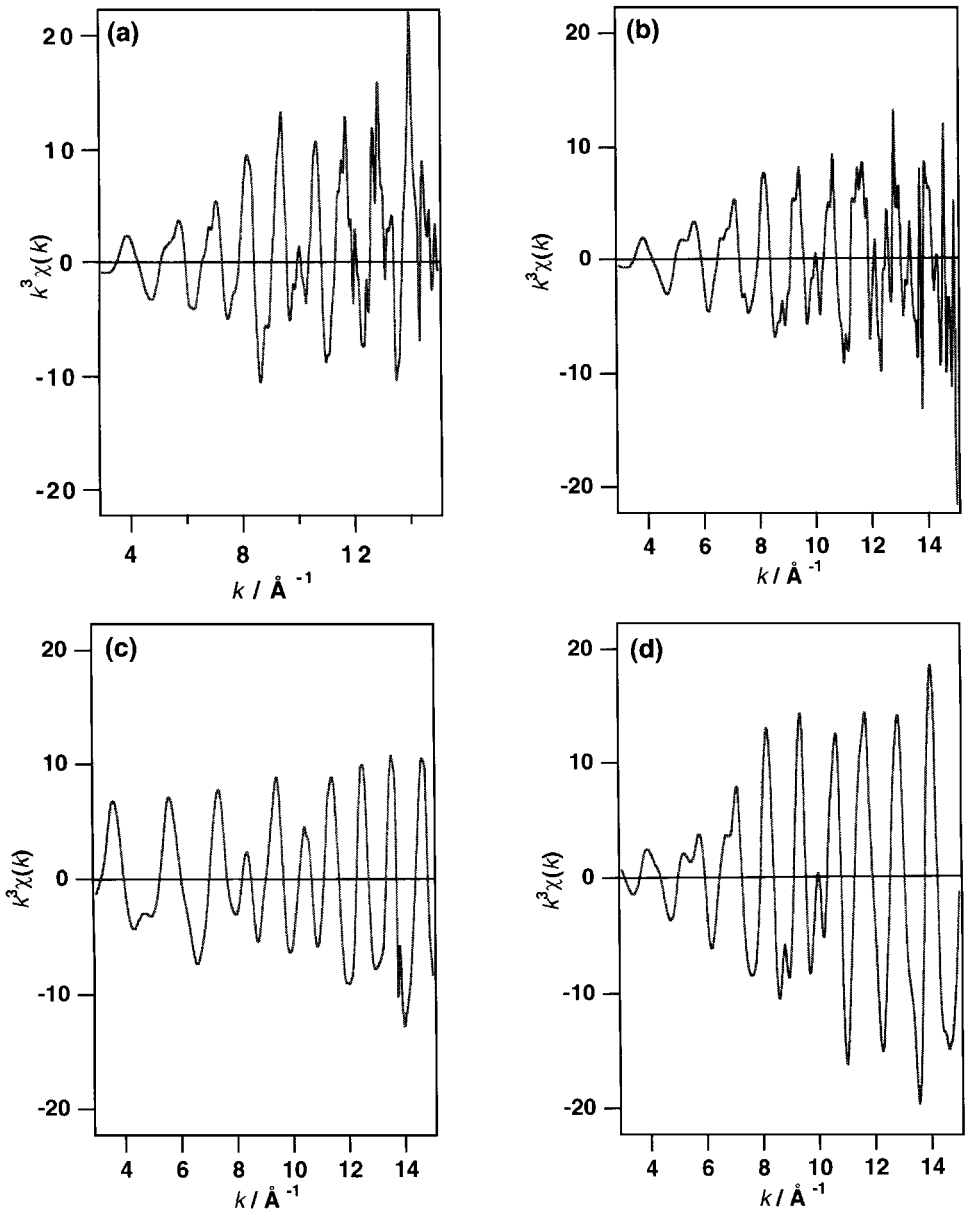

FIG. 3. Pt L_3-edge k^3-weighted EXAFS of (a) oxidized $Pt/SO_4^{2-}-ZrO_2$, (b) reduced $Pt/SO_4^{2-}-ZrO_2$, (c) PtO_2, and (d) Pt foil.

the peaks at 2.2 and 2.6 Å due to the scattering by neighboring Pt atoms. The peak at 2.2 Å is caused by nonlinear parameters (phase shift, back-scattering amplitude) of platinum and called a lobe. The Fourier transform of Pt L_3 edge k^3-weighted EXAFS for PtO_2 exhibits the peaks at 1.7 and 3.0 Å. The peaks at 1.7 and 3.0 Å are due to the Pt–O shell and Pt–O–Pt shell, respectively.

Both oxidized $Pt/SO_4^{2-}-ZrO_2$ and reduced $Pt/SO_4^{2-}-ZrO_2$ exhibit the peaks at 2.2 and 2.6 Å. The peak positions are the same as those observed for Pt foil. However, the peak heights for oxidized $Pt/SO_4^{2-}-ZrO_2$ and reduced $Pt/SO_4^{2-}-ZrO_2$ are less than half that for Pt foil. Small Pt–Pt scattering peaks for both oxidized $Pt/SO_4^{2-}-ZrO_2$ and reduced $Pt/SO_4^{2-}-ZrO_2$ indicates that the size of metallic Pt is small.

In addition to the Pt–Pt scattering peaks at 2.2 and 2.6 Å, a peak is observed in the range of 1–2 Å for both oxidized $Pt/SO_4^{2-}-ZrO_2$ and reduced $Pt/SO_4^{2-}-ZrO_2$, although the peak is not distinctive. The peak position is the same as that found for PtO_2. Unlike PtO_2, no peak appeared at 3.0 Å. To clarify as to whether the peak ascribed to Pt–O shell exists or not, the Fourier transforms of Pt L_3-edge k^3-weighted EXAFS (real part and imaginary part) are shown in Fig. 6 in an expanded scale of R. By the curves for the imaginary part shown in dotted line, it is clearly shown that the peak at about 1.7 Å is observed not only for PtO_2 but also for

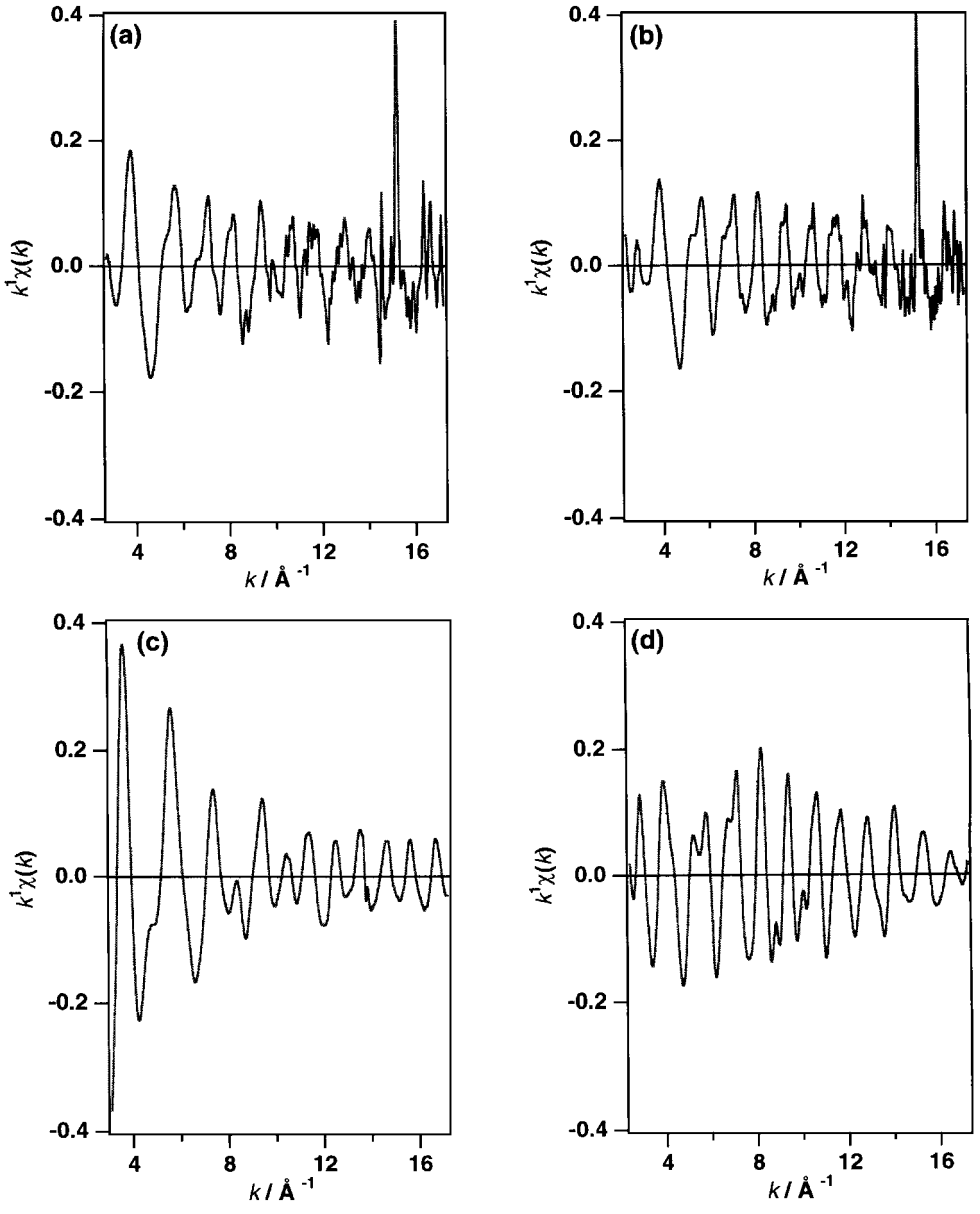

FIG. 4. Pt L_3-edge k^1-weighted EXAFS of (a) oxidized Pt/SO_4^{2-}–ZrO_2, (b) reduced Pt/SO_4^{2-}–ZrO_2, (c) PtO_2, and (d) Pt foil.

both oxidized Pt/SO_4^{2-}–ZrO_2 and reduced Pt/SO_4^{2-}–ZrO_2. The order of the intensity of the peak at 1.7 Å is PtO_2 > oxidized Pt/SO_4^{2-}–ZrO_2 > reduced Pt/SO_4^{2-}–ZrO_2. Consequently, it is indicated that Pt–O shells are present in oxidized Pt/SO_4^{2-}–ZrO_2 and reduced Pt/SO_4^{2-}–ZrO_2 and that the cation/metal ratio is lower for reduced Pt/SO_4^{2-}–ZrO_2 than for oxidized Pt/SO_4^{2-}–ZrO_2.

The presence of Pt–O shell (low Z contribution) in the both oxidized Pt/SO_4^{2-}–ZrO_2 and reduced Pt/SO_4^{2-}–ZrO_2 can be further demonstrated by applying a Fourier transform of k^1-weighted EXAFS which is sensitive to the low Z elements. The Fourier transforms of Pt L_3-edge k^1-weighted EXAFS of the Pt/SO_4^{2-}–ZrO_2, Pt foil and PtO_2 is shown in Fig. 7. The Fourier transforms of Pt L_3-edge k^1-weighted EXAFS for both oxidized Pt/SO_4^{2-}–ZrO_2 and reduced Pt/SO_4^{2-}–ZrO_2 exhibit the peaks at 1.7 Å. PtO_2 also exhibits the peaks at 1.7 Å, while Pt foil does not exhibit this peak. This peak is due to Pt–O shell.

For quantitative analysis of these spectra, the main peak of each transform was isolated, and the inverse Fourier was transformed to k space. The best fit EXAFS parameters (N = coordination number, R = distance, Debye–Waller factor) of the Pt–Pt shell and Pt–O shell for the oxidized Pt/SO_4^{2-}–ZrO_2, reduced Pt/SO_4^{2-}–ZrO_2, Pt foil, and PtO_2 are summarized in Table 1 (k^3-weighting) and Table 2 (k^1-weighting). The Fourier fitted EXAFS spectra

TABLE 1

EXAFS Parameters of Pt–Pt Shell and Pt–O Shell

Sample	Coordination	C. N.	R/Å	$\Delta\sigma^2/Å^2 \times 10^{-3}$
Reduced	Pt–Pt	7.8 ± 1.4	2.78 ± 0.01	2.2 ± 0.8
	Pt–O	2.2 ± 0.8	2.28 ± 0.03	8.4 ± 2.0
Oxidized	Pt–Pt	6.5 ± 1.3	2.77 ± 0.02	2.2 ± 0.8
	Pt–O	3.3 ± 1.1	2.25 ± 0.03	5.0 ± 2.5
Pt foil	Pt–Pt	12	2.77	0

Note. All model fits used a k^3-weighting in the range of R 1.2–3.4 Å.

reproduced by use of the EXAFS parameters in Tables 1 and 2 are shown in Figs. 8 and 9 for the oxidized $Pt/SO_4^{2-}-ZrO_2$ and reduced $Pt/SO_4^{2-}-ZrO_2$. The presence of the Pt–O shell indicates that a part of platinum on the $SO_4^{2-}-ZrO_2$ support is in the form of PtO_x. The average coordination numbers of Pt–Pt shell of the oxidized $Pt/SO_4^{2-}-ZrO_2$ and reduced $Pt/SO_4^{2-}-ZrO_2$ are smaller than the value of 12 which is the average coordination number for Pt foil. When the oxidized $Pt/SO_4^{2-}-ZrO_2$ is treated with hydrogen at 623 K, the average coordination number (k^3-weighting) of the Pt–Pt shell increased from 6.5 to 7.8, while that of the Pt–O shell decreased from 3.3 to 2.2. The coordination numbers of both the Pt–Pt shell and the Pt–O shell for k^1-weighting analysis are close to those obtained by k^3-weighting analysis. These results indicate that a part of the Pt oxide species was reduced to Pt metal by hydrogen treatment. However, it should be noted that Pt–O shells still remain, even after hydrogen treatment at 623 K. The platinum particle size is estimated from the obtained coordination number N for the Pt–Pt shell according to the method proposed by Greegor and Lytle (30), assuming the spherical particle of the face-centered cubic (fcc) packing. For both samples, the diameters of the particle are estimated to be 30–40 Å. This value is slightly smaller than the mean particle size of platinum (50 ± 5 Å) on $SO_4^{2-}-ZrO_2$ (Pt 5 wt%) determined by TEM (8).

DISCUSSION

The intensities of the white lines for both oxidized $Pt/SO_4^{2-}-ZrO_2$ and reduced $Pt/SO_4^{2-}-ZrO_2$ are higher than

TABLE 2

EXAFS Parameters of Pt–Pt Shell and Pt–O Shell

Sample	Coordination	C. N.	R/Å	$\Delta\sigma^2/Å^2 \times 10^{-3}$
Reduced	Pt–Pt	7.2 ± 1.5	2.78 ± 0.01	1.5 ± 1.1
	Pt–O	2.4 ± 0.7	2.25 ± 0.03	6.3 ± 1.8
Oxidized	Pt–Pt	7.0 ± 1.2	2.78 ± 0.02	2.1 ± 0.9
	Pt–O	3.3 ± 0.7	2.26 ± 0.02	5.0 ± 2.1

Note. All model fits used a k^1-weighting in the range of R 1.0–3.3 Å.

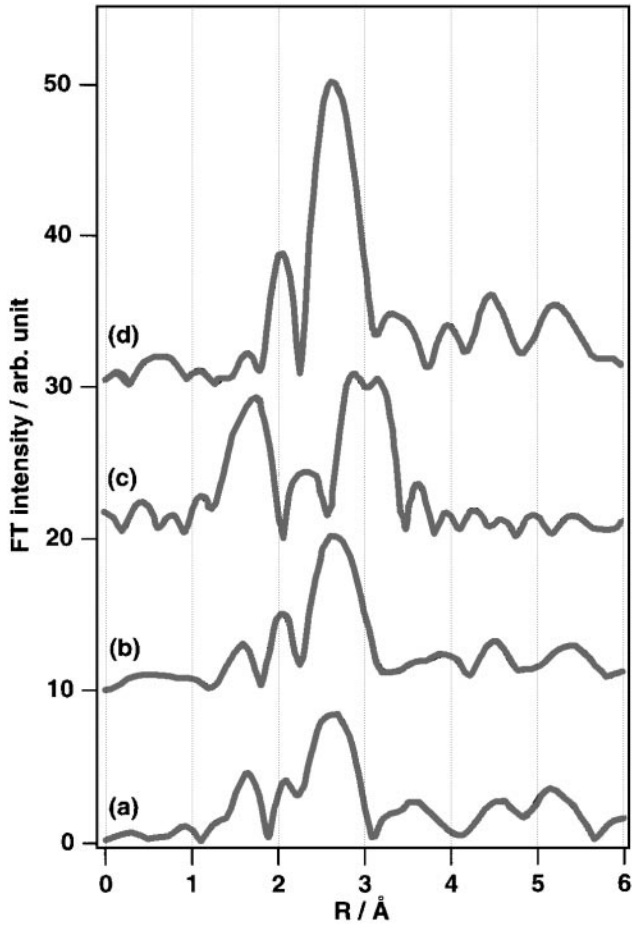

FIG. 5. Fourier transform of EXAFS (k^3, $\Delta k = 3.5$–13.5 Å^{-1}) of (a) oxidized $Pt/SO_4^{2-}-ZrO_2$, (b) reduced $Pt/SO_4^{2-}-ZrO_2$, (c) PtO_2, and (d) Pt foil.

that for Pt foil, but lower than that for PtO_2 in both normalized Pt L_3 and L_2-edge XANES. Therefore, the numbers of unoccupied 5*d* orbitals of platinum of both oxidized $Pt/SO_4^{2-}-ZrO_2$ and reduced $Pt/SO_4^{2-}-ZrO_2$ are larger than that of Pt foil, but smaller than that of PtO_2. It is indicated that the platinum in $Pt/SO_4^{2-}-ZrO_2$ is electron deficient. The electron deficiency of the supported platinum suggests the coexistence of Pt metal with Pt cations and/or the electron transfer from the platinum particles to support. The intensity of the white line decreased on hydrogen treatment at 623 K, suggesting that a part of the platinum is reduced to Pt metal.

The oscillations by XANES at high energy side of the absorption edge for both oxidized $Pt/SO_4^{2-}-ZrO_2$ and reduced $Pt/SO_4^{2-}-ZrO_2$ are closer to that of Pt foil rather than that of PtO_2. This indicates that the state of most platinum on the $SO_4^{2-}-ZrO_2$ is metallic. The intensity of oscillation is much lower for both oxidized $Pt/SO_4^{2-}-ZrO_2$ and reduced $Pt/SO_4^{2-}-ZrO_2$ than for Pt foil. Reduced oscillation can be seen in the XANES for small platinum

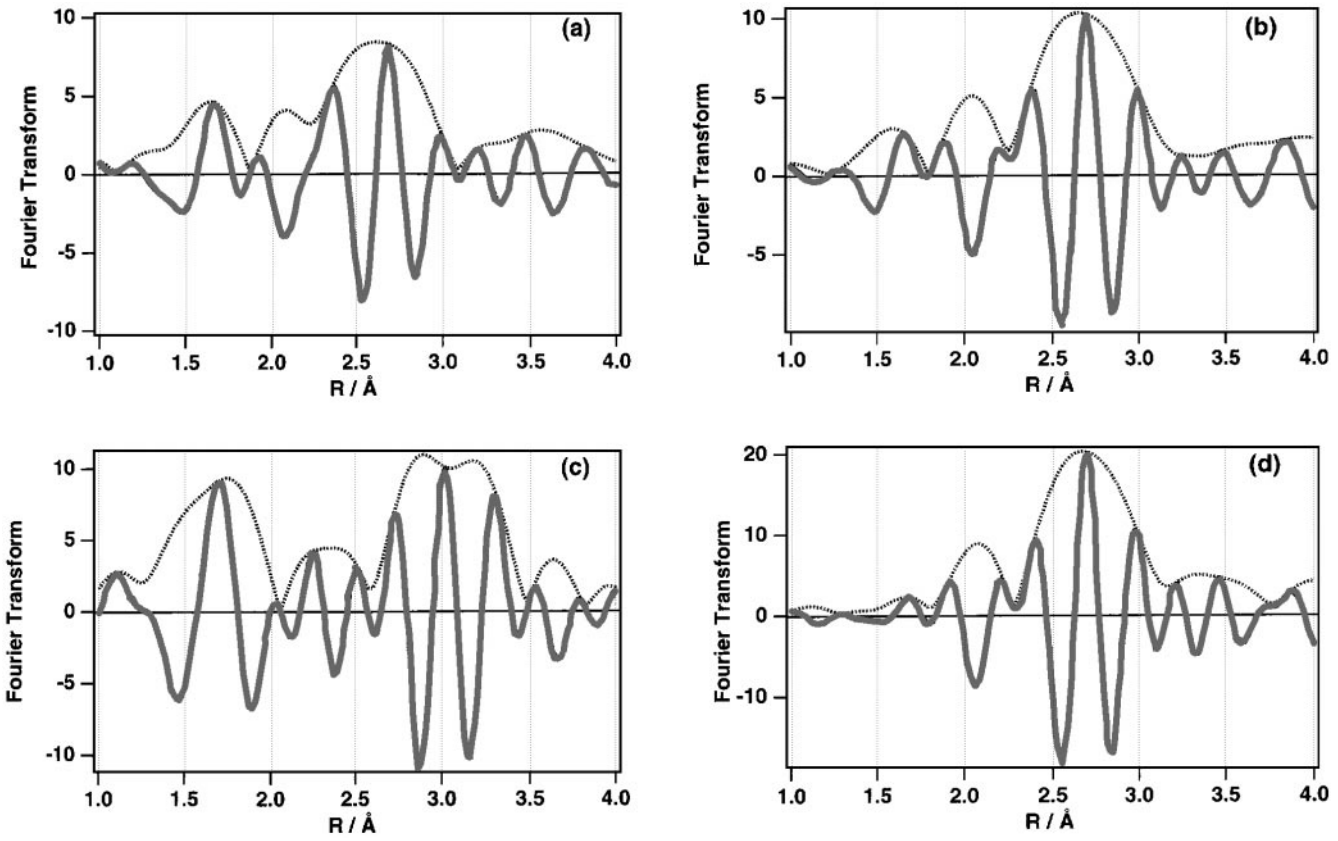

FIG. 6. Fourier transform of EXAFS ((k^3, $\Delta k = 3.5$–13.5 Å^{-1}), expanded view of Fig. 5 between 1.0–4.0 Å) of (a) oxidized Pt/SO_4^{2-}−ZrO_2, (b) reduced Pt/SO_4^{2-}−ZrO_2, (c) PtO_2, and (d) Pt foil; (solid line) real part; (dotted line) imaginary part.

particles as compared with Pt foil (15, 31). A low intensity of oscillation is attributed to a smaller coordination number of Pt for both oxidized Pt/SO_4^{2-}−ZrO_2 and reduced Pt/SO_4^{2-}−ZrO_2 than for Pt foil (Tables 1 and 2). A low intensity may also be caused by the superposition of the platinum metallic phase and the oxide phase. Mixing a considerable amount of the platinum oxide phase with the Pt metallic phase would make the spectrum unclear. The reproduction of XANES spectra (Fig. 2) obtained by fitting XANES of both Pt foil and PtO_2 indicates that about 60% of the platinum is metallic in oxidized Pt/SO_4^{2-}−ZrO_2 and that about 80% of the platinum is metallic in reduced Pt/SO_4^{2-}−ZrO_2. Inconsistent with this result and the white line height, the average coordination number of the Pt–Pt shell for the reduced Pt/SO_4^{2-}−ZrO_2 determined by curve-fitting analysis increases on hydrogen treatment. However, the coordination number of the Pt–Pt shell for the reduced Pt/SO_4^{2-}−ZrO_2 is smaller than that of Pt foil.

Zhao *et al.* reported that Pt is completely in a metallic state following calcination of Pt/SO_4^{2-}−ZrO_2 in air at 998 K for 2 h and that the valence state of Pt does not change during use as a catalyst for hydrocarbon conversion at 423 K under hydrogen pressure (32). They claimed that the average coordination number of platinum is about 12. In our present results, however, the average coordination numbers of Pt–Pt shell of both oxidized Pt/SO_4^{2-}−ZrO_2 and reduced Pt/SO_4^{2-}−ZrO_2 were about 7. The difference may be caused by the following two reasons. First, since their sample was oxidized at a high temperature of 998 K in air, Pt was reduced to the metallic state by means of decomposition of the sulfate ions and the diameter of platinum particles was increased as a result of aggregation (sintering). Second, the magnitude of the white line of Pt foil reported in their paper is larger than that of our results. This suggests that their Pt foil might be oxidized to some extent and that the EXAFS parameters were different from those for Pt metal. Recently, Tabara and Davis reported that XANES of Pt/SO_4^{2-}−ZrO_2 (Pt 0.74 wt%, S 2.1 wt%) calcined at 873 K for 2 h in air is similar to that of PtO_2 (33). This result suggests that state of platinum on SO_4^{2-}−ZrO_2 is different from the metallic state.

Sayari and Dicko proposed on the basis of XPS, TPR, and XRD that Pt is metallic even after calcination in air (12, 13). Paál *et al.* reported on the basis of XPS that a part of the surface platinum on SO_4^{2-}−ZrO_2 is sulfided (10). Iglesia *et al.* (11) reported that Pt is sulfided in Pt/SO_4^{2-}−ZrO_2 after

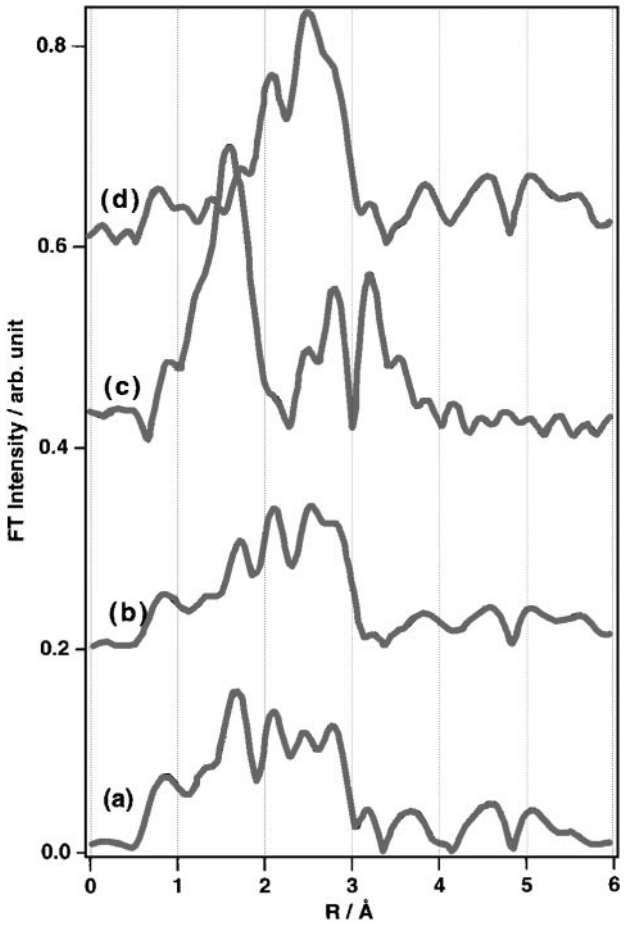

FIG. 7. Fourier transform of EXAFS (k^1, $\Delta k = 4$–12 Å^{-1}) of (a) oxidized $Pt/SO_4^{2-}-ZrO_2$, (b) reduced $Pt/SO_4^{2-}-ZrO_2$, (c) PtO_2, and (d) Pt foil.

reduction with hydrogen at 473 K. We reported that most of the surface platinum on the $SO_4^{2-}-ZrO_2$ (5 wt% Pt) is in a mainly cationic state, even after hydrogen treatment at 673 K, on the basis of XPS and TPR and that the activity of the $Pt/SO_4^{2-}-ZrO_2$ catalyst for hydrogenation is negligibly small as compared to that of Pt/ZrO_2 (2, 4, 5). In addition, CO molecules are not adsorbed on the $Pt/SO_4^{2-}-ZrO_2$ reduced at 623 K (5). Our previous *in situ* XPS investigation showed that most sulfur exist as S^{6+} after hydrogen treatment at 623 K (5). Therefore, the possibility of the PtS (the valence of the sulfur of PtS is considered to be 2−) formation on the surface platinum on the $SO_4^{2-}-ZrO_2$ after hydrogen treatment at 623 K is expected to be small. In addition, the previous TPR profile indicates a low reduction rate for the $Pt/SO_4^{2-}-ZrO_2$ as compared with Pt/ZrO_2 (5). The TPR profile measured on the present $Pt/SO_4^{2-}-ZrO_2$ was essentially the same as that reported previously on the $Pt/SO_4^{2-}-ZrO_2$ containing 5 wt% Pt. The hydrogen consumption peak appeared at a higher temperature for $Pt/SO_4^{2-}-ZrO_2$ than for Pt/ZrO_2. The low reduction rate for the $Pt/SO_4^{2-}-ZrO_2$ suggests the incomplete reduction of the platinum particles on the $SO_4^{2-}-ZrO_2$. Since it is expected that part of platinum particles are oxidized after calcination at 873 K and since hydrogen consumption could not be seen below 700 K in the TPR profile, the unreduced platinum exists as platinum oxide (PtO_x) after hydrogen treatment at 623 K. The presence of the platinum cations was evidenced by the XPS measurement on the $Pt/SO_4^{2-}-ZrO_2$ after hydrogen treatment (2, 4). The observed electron deficiency of the platinum on the $SO_4^{2-}-ZrO_2$ must be due to the coexistence of Pt metal with unreduced platinum oxide rather than the electron transfer from the metallic platinum particles to the support.

In the Fourier transforms of Pt L_3-edge k^3-weighted (emphasizing the Pt–Pt contribution) EXAFS of both oxidized

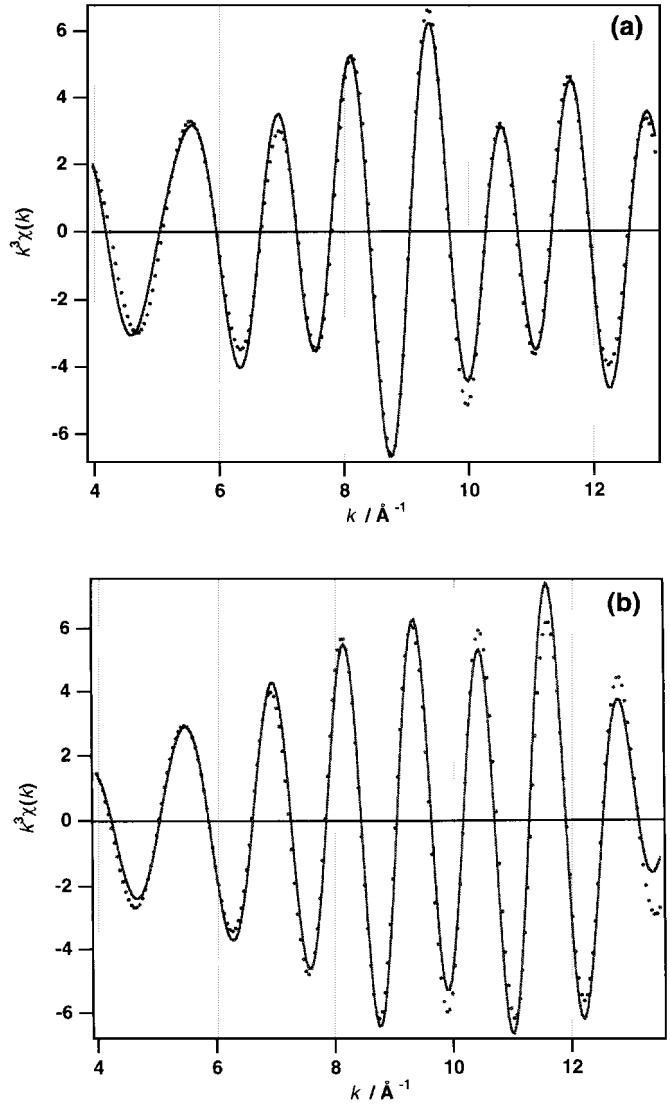

FIG. 8. Fourier-fitted EXAFS spectrum reproduced by use of the parameters in Table 1 (k^3-weighting) of (a) oxidized $Pt/SO_4^{2-}-ZrO_2$, (b) reduced $Pt/SO_4^{2-}-ZrO_2$; (solid line) experimental EXAFS; (dotted line) fitted model.

Pt/SO_4^{2-}–ZrO_2 and reduced Pt/SO_4^{2-}–ZrO_2, two main peaks are observed at 2.6 and 1.7 Å. Since the peak ascribed to Pt–Pt scattering in Pt foil appears at 2.6 Å, the peak at 2.6 Å is due to the scattering by neighboring Pt atoms. The presence of this peak indicates the presence of Pt metallic phase, although the intensity of the peak is less than half that for Pt foil. The low intensity of the peak indicates that small metallic Pt particles are formed on SO_4^{2-}–ZrO_2. The peak at 1.7 Å is absent in Fourier transforms of both k^1 and k^3-weighted EXAFS of Pt foil, but is observed in that of PtO_2. In the Fourier transforms of Pt L_3-edge k^1-weighted (emphasizing low Z element contribution) EXAFS, the relative intensity of the peak at 1.7 Å to the peak at 2.6 Å is emphasized, however, it is de-emphasized in the Fourier transforms of Pt L_3-edge k^3-weighted EXAFS. This peak is due to the Pt–O shell (low Z element contribution). The peak at 1.7 Å in the Fourier transforms of Pt L_3-edge EXAFS of both oxidized Pt/SO_4^{2-}–ZrO_2 and reduced Pt/SO_4^{2-}–ZrO_2 is caused by the Pt–O shell. The presence of the Pt–O shell indicates that a Pt oxide phase is present in both oxidized Pt/SO_4^{2-}–ZrO_2 and reduced Pt/SO_4^{2-}–ZrO_2. Despite the appearance of the peak at 1.7 Å, the Pt–Pt scattering peak at 3.0 Å for the configuration of Pt–O–Pt was not observed. This implies that the Pt–O–Pt configuration is absent or that the configuration is disordered. The absence of the Pt–O–Pt shell suggests that the Pt oxide phase is not present as bulk Pt oxide. One of the possible forms of the Pt oxide is a thin layer of Pt oxide.

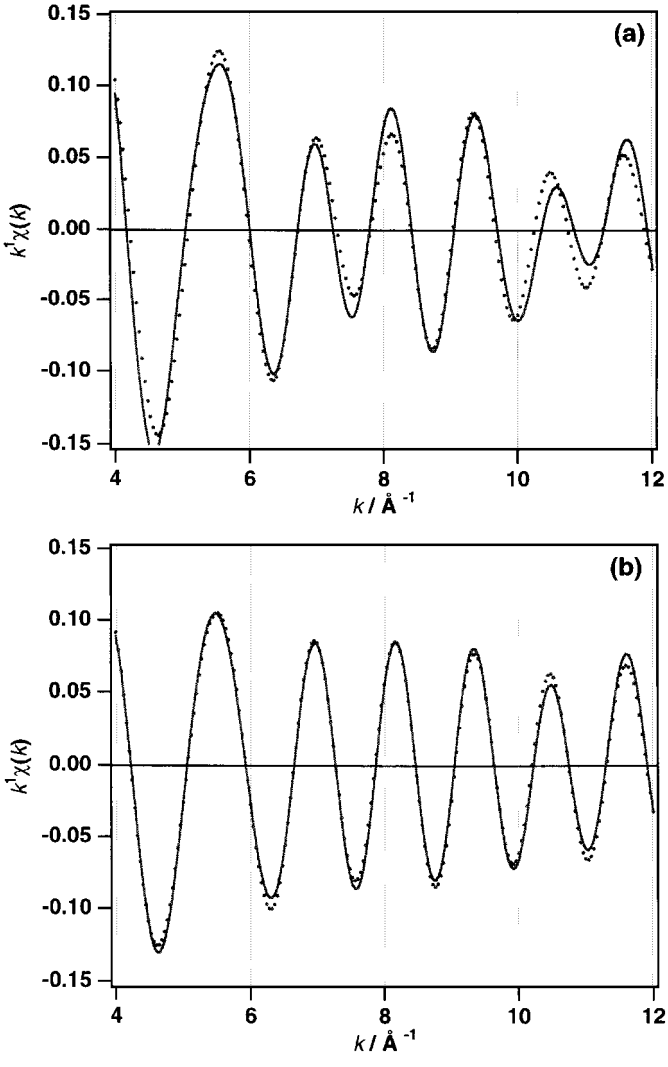

FIG. 9. Fourier-fitted EXAFS spectrum reproduced by use of the parameters in Table 2 (k^1-weighting) of (a) oxidized Pt/SO_4^{2-}–ZrO_2, (b) reduced Pt/SO_4^{2-}–ZrO_2; (solid line) experimental EXAFS; (dotted line) fitted model.

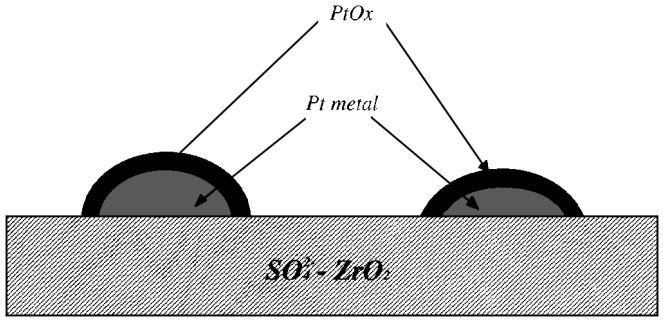

FIG. 10. Proposed model of platinum over SO_4^{2-}–ZrO_2.

The proposed model for the Pt/SO_4^{2-}–ZrO_2 after reduction with hydrogen at 623 K is illustrated in Fig. 10. Platinum on the SO_4^{2-}–ZrO_2 is in such a state that metallic Pt particles are covered with the thin layer of platinum oxide. XPS is a surface analysis technique and XRD is a bulk analysis technique. The model can explain that Pt cations are dominantly detected by XPS (5, 7) while metallic platinum particles are detected by XRD (10, 11). The model also explains that the Pt/SO_4^{2-}–ZrO_2 does not absorb the CO molecule and exhibits a low hydrogenation ability.

ACKNOWLEDGMENTS

The X-ray absorption experiments were performed under the approval of the Photon Factory Program Advisory Committee (Proposal 90-154). This work is partly supported by a Grant in Aid for Scientific Research from the Ministry of Education, Science, Sports and Culture, Japan.

REFERENCES

1. Hosoi, T., Shimadzu, T., Ito, S., Baba, S., Takaoka, H., Imai, T., and Yokoyama, N., *Prepr. Symp. Div. Petr. Chem. Am. Chem. Soc.*, 562 (1988).
2. Ebitani, K., Konishi, J., and Hattori, H., *J. Catal.* **130**, 257 (1991).
3. Ebitani, K., Tsuji, J., Hattori, H., and Kita, H., *J. Catal.* **135**, 609 (1992).
4. Shishido, T., and Hattori, H., *J. Catal.* **161**, 194 (1996).
5. Ebitani, K., Konno, H., Tanaka, T., and Hattori, H., *J. Catal.* **135**, 60 (1992).
6. Sang, X., and Sayari, A., *Catal. Rev.-Sci. Eng.* **38**, 329 (1996).
7. Ebitani, K., Konno, H., Tanaka, T., and Hattori, H., *J. Catal.* **143**, 322 (1992).

8. Ebitani, K., Tanaka, T., and Hattori, H., *Appl. Catal. A: General* **102**, 79 (1993).
9. Tanaka, T., Shishido, T., Hattori, H., Ebitani, K., and Yoshida, S., *Physica B* **208/209**, 649 (1995).
10. Paál, M., Muhler, M., and Schröl, R., *J. Catal.* **143**, 318 (1993).
11. Iglesia, E., Doled, S. L., and Kramer, G. M., *J. Catal.* **144**, 238 (1993).
12. Dicko, A., Song, X., Adnot, A., and Sayari, A., *J. Catal.* **150**, 254 (1994).
13. Sayari, A., and Dicko, A., *J. Catal.* **145**, 561 (1994).
14. Teo, B. K., *in* "EXAFS: Basic Principles and Data Analysis." Springer-Verlag, Berlin, 1986.
15. Short, D. R., Mansour, A. N., Cook, J. W., Jr., Sayer, D. E., and Katzer, J. R., *J. Catal.* **82**, 299 (1983).
16. Koningsberger, D. C., Martens, J. H. A., Prins, R., Short, D. R., and Sayer, D. E., *J. Phys. Chem.* **90**, 3047 (1986).
17. Martens, J. H. A., Prins, R., Zandbergen, H., and Koningsberger, D. C., *J. Phys. Chem.* **92**, 1903 (1988).
18. Via, G. H., Sinfelt, J. H., and Lytle, F. W., *J. Chem. Phys.* **71**, 690 (1979).
19. Brown, M., Peiels, R. E., and Stern, E. A., *Phys. Rev. B* **15**, 738 (1977).
20. Bart, J. C. J., *Adv. Catal.* **34**, 203 (1986).
21. Lytle, F. W., *J. Catal.* **43**, 376 (1976).
22. Lytle, F. W., Wei, P. S. P., Greegor, R. B., Via, G. H., and Sinfelt, J. H., *J. Chem. Phys.* **70**, 4849 (1979).
23. Mansour, A. N., Cook, J. W., Jr., and Sayers, D. E., *J. Phys. Chem.* **88**, 2330 (1984).
24. Mansour, A. N., Cook, J. W., Jr., Sayers, D. E., Emrich, R. J., and Katzer, J. R., *J. Catal.* **89**, 462 (1984).
25. Yoshida, S., and Tanaka, T., *Adv. in X-ray Chem. Anal. Jpn.* **19**, 97 (1988).
26. McMaster, W. H., Kerr Del Grande, N., Mallet, J. H., and Hubell, J. H., "Composition of X-ray Cross Sections." National Technical Information Service, Springfield, 1969.
27. Tanaka, T., Yamashita, H., Tsuchitani, R., Funabiki, T., and Yoshida, S., *J. Chem. Soc., Faraday Trans. 1* **84**, 2987 (1988).
28. Sayer, D. E., Stern, E. A., and Lytle, F. W., *Phys. Rev. Lett.* **27**, 1204 (1971).
29. Koningsberger, D. C., Stereochemistry and electronic structure. XAFS spectroscopy: Data-analysis and applications, *in* "Physics and Chemistry of Solids" (J. Baruchel, J. L. Hodeau, M. S. Lehmann, J. R. Regard, and C. Schlenker, Eds.), Vol. II, Chap. X, p. 213. Springer-Verlag, Berlin, 1993. [Hercules Course]
30. Greegor, R. B., and Lytle, F. W., *J. Catal.* **63**, 476 (1980).
31. Samant, M. G., and Boudart, M., *J. Phys. Chem.* **95**, 4070 (1991).
32. Zhao, J., Huffman, G. P., and Davis, B. H., *Catal. Lett.* **24**, 385 (1994).
33. Tabora, J. E., and Davis, R. J., *J. Catal.* **162**, 125 (1996).